Surface & Coatings Technology 258 (2014) 102–107

Contents lists available at ScienceDirect

Surface & Coatings Technology

journal homepage: www.elsevier.com/locate/surfcoat

# Microstructure, hardness and corrosion behaviour of Ti/TiN multilayer coatings produced by plasma activated EB-PVD

Dapeng Zhou [a], Hui Peng [a,*], Liu Zhu [a,b], Hongbo Guo [a], Shengkai Gong [a]

[a] School of Materials Science and Engineering, Beihang University, No. 37 Xueyuan Road, Beijing 100191, China
[b] School of Mechanical Engineering, Taizhou University, No. 1139, Shifu Road, Taizhou, Zhejiang 317000, China

ARTICLE INFO

*Article history:*
Received 17 May 2014
Accepted in revised form 25 September 2014
Available online 12 October 2014

*Keywords:*
Multilayer
Plasma activation
Corrosion
Hardness
Ti/TiN
EB-PVD

ABSTRACT

Compressor blades used in gas turbine engines for marine applications must work in harsh environment such as erosion and corrosion. Multilayer nitride coatings produced by physical vapour deposition (PVD) have exhibited promising potential in improving the corrosion resistance. In this paper, three types of Ti/TiN multilayer coatings with different thickness ratios (M1: 10 nm/40 nm, M2: 20 nm/80 nm, M3: 30 nm/80 nm) were deposited onto 1Cr11Ni2W2MoV stainless steel substrates by plasma activated electron beam physical vapour deposition (EB-PVD). The microstructure, hardness and corrosion behaviour of the Ti/TiN multilayer coatings and TiN single layer coating were comparatively studied. The columnar grain growth of the TiN single layer coating was suppressed by the introduction of the Ti metallic sublayers. With the increase of the Ti sublayer thickness, the characteristics of the layered microstructure became more apparent. The substrates coated with Ti/TiN multilayer coatings exhibited better corrosion resistance (maximum 87% protection efficiency for M3) and higher hardness value (maximum 34.1 GPa for M1) than those coated with TiN single layer.



## 1. Introduction

Serving environment is a key factor that determines the reliability and performances of a gas turbine compressor. It has been shown that the marine environment can accelerate the corrosion failure of compressor blades as a result of the attack of the moisture containing salts and acids [1,2]. Besides, sands and other particles ingested by the engines can also lead to blades erosion. The synthetic effect of corrosion and erosion can result in accelerated damage of the blades metal, leading to an increased fuel consumption, efficiency loss, decreased lifetime, or even disasters.

One effective method to prevent the corrosion/erosion induced damage of blade is to apply PVD nitride coatings, which possess the ideal combination of good adhesion, sufficient plasticity, high hardness and high corrosion/erosion resistance [3]. The application of TiN coatings is a proven process which protects the blades from corrosion/erosion attack from dust/debris and water droplets in the inlet air [4]. Moreover, multi-element nitride coatings, such as TiAlN [5], TiZrN [6], and TiSiCN [7] have been investigated for better performance.

Another optimization of nitride coatings for substrate protection is the multilayer structure consisting of thin layers with different materials. Feuerstein et al. have reported a substoichiometric $TiN/TiN_{1-x}$ "24k Type II™" multilayer coating with improved erosion resistance compared to conventional TiN coatings. The improved performance is due to coating's multilayer structure which can increase hardness and toughness of the coating [8]. Multilayer structure was also used to enhance mechanical and tribological properties of coatings which were applied on cutting tools [9]. Adopting multilayer structure is a proved effective way to optimize properties of coatings.

The commonly used deposition methods for multilayer nitride coatings are arc ion plating (AIP) and reactive magnetron sputtering (MP). It is easily to get a reliable control of coating thickness and microstructure with both methods. However, defects within the AIP coatings, such as macroparticle contamination which is inherent to the unfiltered cathodic arc process, can lead to a premature corrosion failure of the coating [10]. In the case of MP coatings, the relatively low deposition rate and low ionization rate make it not a cost effective way for applying high quality thick nitride coatings onto compressor blades. It is worth mentioning that new developments of AIP and MP are emerging, including filtered cathodic arc [11], pulse enhanced electron emission (P3e™) [12], and HIPIMS [13], aiming to improve both the coating rate and quality.

Electron beam-physical vapour deposition (EB-PVD) is a superior vacuum coating technology with the merits of high deposition rate and free of macroparticles. Moreover, compound coatings can easily be deposited by EB-PVD when assisted with plasma activation [14]. This makes plasma activated EB-PVD an appropriate method for depositing high quality protective coatings onto compressor blades. A so-called reactive ion coating (RIC™) process, in which plasma is activated by electrons ejected from Tungsten filaments, has been developed by Liburdi Inc. for compressor blades protection [15]. Metzner et al. performed

* Corresponding author. Tel.: +86 10 8231 7117; fax: +86 10 8233 8200.
*E-mail address:* penghui@buaa.edu.cn (H. Peng).

http://dx.doi.org/10.1016/j.surfcoat.2014.09.058
0257-8972/

the plasma activated EB-PVD in another way, by burning a spotless arc discharge (SAD process) [16]. The SAD exhibits an extremely high ionization rate (up to 60%) [17], and has been used for industrial deposition of Ti and its compound coatings in a steady, long-term mode.

In this work, we deposited Ti/TiN multilayer coatings onto stainless steel substrates by plasma activated EB-PVD (SAD process). The microstructure, hardness and corrosion behaviour of the coatings were investigated.

## 2. Experimental

### 2.1. Materials and coating preparation

The substrate material is 1Cr11Ni2W2MoV martensitic stainless steel (nominal compositions in wt.%: C 0.1–0.16, Cr 10.5–12, Ni 1.4–1.8, W 1.5–2, Mo 0.35–0.5, V 0.18–0.30, Mn 0.6, Si 0.6, S 0.02 and P 0.03), which is commonly used for compressor blades of gas turbine engines. The 1Cr11Ni2W2MoV rod was machined to disc-shaped specimens with a diameter of 25 mm and a thickness of 3 mm. Meanwhile, HSS and austenitic stainless steel substrates were also coated for fracture observation and TEM observation. Prior to coating deposition, all the substrate surfaces were mirror polished, and then were ultrasonically cleaned in the acetone medium and thoroughly dried.

Depositions were carried out in the SAD process, the principle of which was demonstrated in Refs. [18,19]. The base pressure in the deposition chamber was ~$10^{-3}$ Pa. The substrates were biassed at −800 V for Ar ion etching at a pressure of 7 Pa for 20 min prior to coating. And then the substrates were bombarded with Ti plasma for 10 min with the same bias voltage. The Ti plasma was generated by a spotless arc discharge (50 V, 100 A) between the molten Ti target (99.9% pure) and the anode. Following Ti ion cleaning, the bias was decreased to −150 V for depositing a 1 μm thick pure Ti as bond coat to improve the interface adhesion. For TiN single layer coating deposition (denoted as S coating), nitrogen with a flow rate of 120 sccm was introduced into the coating chamber to a pressure of ~$2 * 10^{-2}$ Pa, and the deposition was lasted for 40 min. For the deposition of Ti/TiN multilayer coatings, a discontinuous nitrogen flow was applied to produce alternating layers of Ti and TiN (without nitrogen for the deposition of Ti sublayer). Three types of Ti/TiN multilayer coatings (denoted as M1, M2 and M3) were produced by periodically turning off the nitrogen flow for 10 s, 20 s and 30 s, respectively. The TiN sublayers within the multilayer coatings were deposited for 30 s in each deposition cycle. During depositions, the substrate temperature was maintained at ~473 K. The power of electron beam for melting the Ti target was ~6 kW (17 kV, 0.35 A).

### 2.3. Evaluation of coating characteristics

The phases of the coatings were investigated by X-ray diffraction (XRD, Bruker D8 Advance) using Cu Kα radiation, which was operated at 40 kV and 40 mA. The scanning angular (2θ) was ranged from 20° to 90° with a scanning speed of 4°/min. The microstructure of the coatings was examined by scanning electron microscope (SEM, FEI Quanta 200F) and transmission electron microscope (TEM, JEM-2100F, capable of performing selected area electron diffraction (SAED)). The fracture sections of the coatings were prepared by fracturing samples in liquid nitrogen. TEM samples were prepared by ion milling with precision ion polishing system (GATAN-691). Corrosion behaviour of the coatings was investigated by potentiodynamic polarization tests in simulated sea water (3.5 wt.% NaCl solution) at 298 K. The corrosion resistance of samples was tested by using a Parstat 2273 potentiostat/galvanostat analyzer (Princeton Applied Research & AMTECT Company). PowerSuite software was used to analyze the electrochemical data. The test appliance was a three-electrode system consisting of a saturated calomel electrode (SCE), a platinum reference electrode and a working electrode (samples). Before testing, the tested samples were stabilized in the electrolyte until the potential change was reduced to below 1 mV/min, and this potential was then taken as the open-circuit potential (OCP). The polarization of the samples was carried out in the range of ±0.9 V above OCP to cover the Tafel region of the polarization. Nanoindentation tests (Nanoindenter XP equipped with Berkovich diamond tip, MTS Systems Corp.) were also performed to measure the hardness and plasticity of the coatings by using continuous stiffness measurement (CSM) method.

## 3. Results and discussion

### 3.1. Microstructure of as-deposited coatings

Fig. 1 shows the typical XRD patterns of S, M1, M2 and M3 coatings. All the coatings exhibit a preferential growth of TiN (111). As shown in Fig. 1, only the signals of TiN and α-Ti phases can be detected in the S coating. After the introduction of Ti sublayers, $Ti_2N$ peaks appear. This result is consistent with other references, in which it was confirmed that the $Ti_2N$ phase was formed at the Ti/TiN interfaces as a transition layer due to the intermediate level of $N_2$ partial pressure just after switching off the nitrogen flow [20]. One thing should be noted is that the Ti (110) peak in Fig. 1 suggests the preferred orientation of the Ti bond coat. However, with continued increase of the deposition of Ti sublayers, the intensity of Ti (101) and Ti (002) peaks becomes stronger and stronger (from M1 to M3), showing a different preferential growth of the Ti sublayers. This might be the textured TiN affects the growth orientation of the subsequent Ti sublayers.

Fig. 2 presents the SEM surface morphology of the as-deposited TiN coating. Compared with AIP coatings [21,22], the coating produced by plasma activated EB-PVD exhibits a smooth surface with no macroparticles can be observed. This is mainly because that the plasma generated in SAD is gained by a diffusive arc with current density of $10^1$–$10^3$ A/cm$^2$, which is much lower than that of a cold cathode arc in AIP [23]. The diffusive arc eliminates the emission of spits and macroparticles, which are usually detrimental to the coating quality. It has been pointed out that reducing coating defects is helpful to prevent corrosion medium from contacting the substrate surface and to delay the occurrence of pitting corrosion [24].

The fractured sections of the coatings are shown in Fig. 3. For all the coatings, the coating/substrate interface exhibits excellent adhesion with no visible delaminating and cracks. The M3 coating reveals a slightly larger thickness (6.3 μm) than that of the other three coatings (4.9 μm, 5.3 μm and 4.6 μm for S, M1 and M2, respectively). This can be partially attributed to the relatively higher volume fraction of the Ti sublayers in the M3 coating. Ti possesses higher deposition rate compared with TiN in the multilayer deposition cycles. The thickness of the

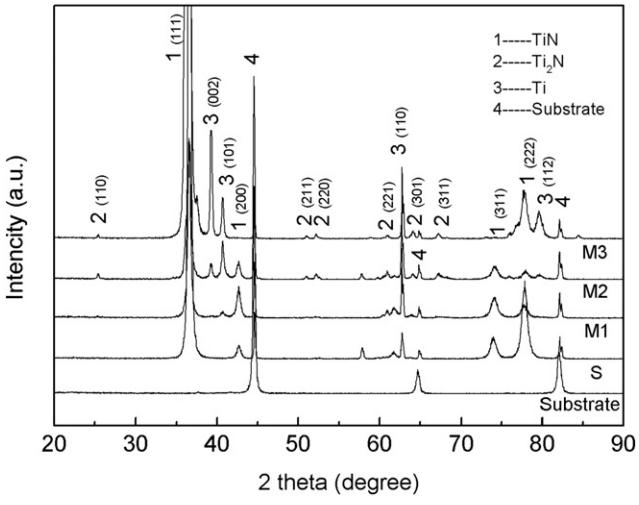


**Fig. 1.** X-ray diffraction patterns of samples S, M1, M2, M3 and substrate.